Published in final edited form as:

Neuron. 2017 May 17; 94(4): 800–808.e4. doi:10.1016/j.neuron.2017.04.041.

CaMKII Autophosphorylation is Necessary for Optimal Integration of Ca^{2+} Signals During LTP Induction but Not Maintenance

Jui-Yun Chang[1,2], **Paula Parra-Bueno**[2], **Tal Laviv**[2], **Erzsebet M. Szatmari**[2], **Seok-Jin R. Lee**[3,4], and **Ryohei Yasuda**[2,3]

[1]Department of Biochemistry, Duke University Medical Center, Durham, NC 27707, USA

[2]Max Planck Florida Institute for Neuroscience, Jupiter, FL 33458, USA

[3]Department of Neurobiology, Duke University Medical Center, Durham, NC 27707, USA

SUMMARY

CaMKII plays a critical role in decoding calcium (Ca^{2+}) signals to initiate long-lasting synaptic plasticity. However, the properties of CaMKII that mediate Ca^{2+} signals in spines remain elusive. Here, we measured CaMKII activity in spines using fast-framing two-photon fluorescence lifetime imaging. Following each pulse during repetitive Ca^{2+} elevations, CaMKII activity increased in a stepwise manner. Thr286 phosphorylation slows the decay of CaMKII and thus, lowers the frequency required to induce spine plasticity by several fold. In the absence of Thr286 phosphorylation, increasing the stimulation frequency results in high peak mutant $CaMKII^{T286A}$ activity that is sufficient for inducing plasticity. Our findings demonstrate that Thr286 phosphorylation plays an important role in induction of LTP by integrating Ca^{2+} signals, and it greatly promotes, but is dispensable for the activation of CaMKII and LTP.

INTRODUCTION

Activation of CaMKII in dendritic spines is considered to be one of the first biochemical steps translating the information encoded in rapid Ca^{2+} elevations (~100 ms) into a long-lasting increase of synaptic strength during LTP and spine enlargement associated with LTP (structural LTP or sLTP) (De Koninck and Schulman, 1998; Lisman et al., 2012; Matsuzaki et al., 2004). CaMKII links Ca^{2+} elevations to downstream cellular targets responsible for LTP and sLTP by phosphorylating diverse substrates (Barria et al., 1997; Murakoshi et al.,

Contact Information: Lead Contact: Ryohei Yasuda (Ryohei.Yasuda@mpfi.org), Max Planck Florida Institute for Neuroscience, One Max Planck Way, Jupiter, FL 33458, USA, Phone: +1-561-972-9202, Fax: +1-561-972-9001.
[4]Present Address: Yonsei University College of Medicine, Seoul, Korea

AUTHOR CONTRIBUTIONS

J.Y.C. and R.Y. designed the experiments. S-J.R.L initiated the project. J.Y.C. performed the majority of experiments. P.P.-B. and T.L. performed the electrophysiological experiments. E.S. performed biochemical experiments. J.Y.C and R.Y. analyzed the data and wrote the paper. All authors discussed the results and commented on the manuscript.

2011; Opazo et al., 2010; Walkup et al., 2015; Yang et al., 2013). At its basal state, CaMKII is locked in an inactive state through the binding of a regulatory segment to its substrate binding site. Upon the influx of Ca^{2+}, Ca^{2+}/calmodulin (Ca^{2+}/CaM) binds to CaMKII and induces its activation. The subsequent autophosphorylation at Thr286 in CaMKIIα (Thr287 in CaMKIIβ), which is located in the mouth of the regulatory segment, prevents the rebinding of the regulatory segment to the kinase domain. This permits an autonomous activity of CaMKII that is independent of Ca^{2+}/CaM binding (Chao et al., 2011; Hanson et al., 1989; Hanson et al., 1994; Lisman et al., 2012). It has been hypothesized that this autonomous activity is the biochemical memory storage for LTP, learning and memory (Lisman et al., 2012). Consistent with the critical role Thr286 phosphorylation in LTP, knock-in mice in which Thr286 of CaMKIIα is mutated to Alanine (*Camk2a*^{T286A}) were impaired in LTP, learning and memory (Giese et al., 1998). However, it was found that the memory deficits in *Camk2a*^{T286A} mice can be overcome by intense training, suggesting that the phosphorylation may be not required for the maintenance of memory once it is established (Irvine et al., 2005). Furthermore, studies using pharmacological or optogenetic inhibitors of CaMKII demonstrated that blocking CaMKII activity before LTP induction abolishes LTP, but inhibiting CaMKII after LTP induction does not reverse LTP, inconsistent with the autonomous CaMKII hypothesis of biochemical memory storage (Buard et al., 2010; Chen et al., 2001; Malinow et al., 1989; Murakoshi et al., 2017; Otmakhov et al., 1997; Sanhueza et al., 2011), but also see (Sanhueza et al., 2007).

More recently, CaMKII activation was directly measured during sLTP of spines using two-photon fluorescence lifetime imaging microscopy (2pFLIM) or ratiometric FRET imaging microscopy in combination with CaMKII activity sensors, Camuiα or its variants (Fujii et al., 2013; Lee et al., 2009; Takao et al., 2005; Yagishita et al., 2014). These sensors measured the conformation change of CaMKII by fluorescence resonance energy transfer (FRET) between fluorophores attached to the two ends of CaMKIIα subunit, and their FRET efficiency was correlated with CaMKII activity (Lee et al., 2009; Takao et al., 2005). The imaging results showed that CaMKII activation rapidly occurs in ~10 s and returns to basal levels within ~1 min during sLTP, suggesting that CaMKII activation is transient (Lee et al., 2009; Yagishita et al., 2014). However, the exact role of Thr286 phosphorylation in CaMKII activation during spine plasticity still remains elusive.

Here, in order to elucidate the biochemical step of CaMKII activation during sLTP of spines, we improved the temporal resolution of fluorescence lifetime imaging to the millisecond range. We found that CaMKII functions as a leaky biochemical integrator of Ca^{2+} signals, and Thr286 phosphorylation critically shapes Ca^{2+} integration. In the absence of Thr286 phosphorylation, CaMKIIα^{T286A} activity decays ~3 fold faster and thus impairs the integration capability of CaMKII. This integration deficit, however, could be overcome by increasing the stimulation frequency which allows the mutant to reach a level sufficient for inducing structural and electrophysiological LTP. Our results indicate that Thr286 autophosphorylation is required for the induction of spine plasticity by facilitating Ca^{2+} integration mediated by CaMKII, but phosphorylation is dispensable for plasticity maintenance.

RESULTS

To investigate the millisecond temporal profile of CaMKII activation in accord with Ca^{2+} transients induced by two-photon glutamate uncaging, we optimized our setup to improve the temporal resolution of 2pFLIM up to 128 ms/frame (32 × 32 pixels) (Figure 1A–1B, S1).

In response to repetitive pulses of two-photon glutamate uncaging in the absence of extracellular Mg^{2+}, Ca^{2+} was elevated to the micromolar level and decayed over ~100 ms (Figure S2). During a typical structural LTP (sLTP) induction protocol consisting of 30 pulses of glutamate uncaging at 0.49 Hz (Lee et al., 2009; Matsuzaki et al., 2004), we observed a rapid and robust activation of CaMKII in stimulated spines. CaMKII activity decayed over tens of seconds (Figure 1A, 1B). The averaged time course of CaMKII activation during sLTP (Figure 1C) showed stepwise increases following each glutamate uncaging pulse until plateauing within ~10 s. After the cessation of glutamate uncaging, CaMKII activity decayed with time constants of τ_{fast} = 6.4 ± 0.7 s (74%) and τ_{slow} = 92.6 ± 50.7 s (26%).

To clarify how CaMKII integrates Ca^{2+} signals, we measured CaMKII activation in response to a single glutamate uncaging pulse (Figure 1D-1F). The time course showed a rapid activation that peaked within 1 s and then decayed over tens of seconds. On average, the time constant of CaMKII activation was 0.3 ± 0.1 s, and the fast decay component was τ_{fast} = 8.2 ± 1.7 s (Figure 1F). Comparing this curve with CaMKII activation during sLTP induction (Figure 1C, Figure S4A), CaMKII appears to linearly summate its activity in response to repetitive glutamate uncaging pulses until reaching its plateau, suggesting that CaMKII activity is modulated by Ca^{2+} elevations and acts as a leaky integrator with time constants of ~6 s and ~1 min (Figure S4A).

The above experiments were performed with relatively long glutamate uncaging pluse (4 – 6 ms) at room temperature (25 ± 0.5°C). We found that a shorter duration of laser pulses (0.5 ms) activated CaMKII in a similar way (Figure S4A). At a near physiological temperature (34–35°C), CaMKII activity decayed faster (τ_{fast} = 1.8 ± 1.6 s (45%) and τ_{slow} = 11.0 ± 19.0 s (55%); Figure S4B, S4C). From these results, the temperature dependency of the decay kinetics in spines was determined to be Q_{10} = 3.6 (τ_{fast}) and 8.4 (τ_{slow}).

CaMKII activity is known to be regulated by autophosphorylation at Thr286 (Lisman et al., 2012). However, the role of Thr286 phosphorylation in the integration of Ca^{2+} signals remains unknown. To address this, we first used the Camuiα mutant in which the phosphorylation site is mutated to alanine (Camuiα^{T286A}), which occludes Thr286 phosphorylation. We compared the activation of the T286A mutant to that of Camuiα^{WT} in response to a single glutamate uncaging pulse (Figure 2A). The activity of CaMKIIα^{T286A} rapidly increased to a level similar to CaMKIIα^{WT}, but decayed with a single component that was ~3 fold faster than CaMKIIα^{WT} (τ_{decay} = 1.9 ± 0.3 s). These results indicate that Thr286 phosphorylation substantially slows the decay of CaMKII activity.

Next, we measured the activity of CaMKIIα^{T286A} during sLTP induction (glutamate uncaging at 0.49 Hz). In contrast to the activation of Camuiα^{WT}, Camuiα^{T286A} failed to accumulate its activity due to rapid decay kinetics (Figure 2B, 2C). CaMKII^{T286A} activity

remained attenuated, activating and decaying in accord with each uncaging pulse (τ_{decay} = 1.9 ± 1.2 s; Figure 2C, Figure S4B). To determine whether activation of Camuiα^{T286A} might be affected by its incorporation into endogenous CaMKII holoenzyme with wild-type CaMKII subunits, we measured Camuiα^{T286A} activation in hippocampal slices from *Camk2a*^{T286A} knock-in mice. In this scenario, Thr286 of all subunits in the holoenzyme are mutated. We observed similar results when using hippocampal slices from *Camk2a*^{T286A} knock-in mice (τ_{decay} = 1.9 ± 0.2 s; Figure S4D, S4E), suggesting that the assembly with wild-type CaMKII subunits does not alter the kinetics of Camuiα^{T286A}.

To further investigate the role of Thr286 phosphorylation, we also imaged the activity of Camuiα^{T286D} phosphomimetic mutant, and Camuiα$^{T286D/T305A/T306A}$, which additionally prevents inhibitory autophosphorylation at Thr305 and Thr306 (Pi et al., 2010b; Shen et al., 2000). Consistent with its constitutively active nature, the basal fluorescence lifetime of Camuiα^{T286D} and Camuiα$^{T286D/T305A/T306A}$ were higher than the maximum activation of Camuiα^{WT} (Figure 2B). This observation suggests pseudo-phosphorylation at Thr286 is sufficient to force CaMKII to adopt an open conformation in the absence of Ca^{2+} elevation. Furthermore, Camuiα^{T286D} and Camuiα$^{T286D/T305A/T306A}$ showed a small, but significant activation by glutamate uncaging, presumably due to the binding of Ca^{2+}/CaM to the subunit (Figure 2D, 2E). While the first uncaging pulse activated all Camuiα variants to a similar degree, the phosphorylation mutants showed markedly less integration of activity compared to WT. The decay time constants, which likely reflects Ca^{2+}/CaM dissociation from pseudo-phosphorylated forms of CaMKII, were 3.0 ± 0.6 s for Camuiα^{T286D} (Figure 2D) and 5.7 ± 0.5 s for Camuiα$^{T286D/T305A/T306A}$ (Figure 2E). The prolonged decay time of Camuiα$^{T286D/T305A/T306A}$ is likely due to the enhanced Ca^{2+}/CaM binding affinity, since Camuiα$^{T305A/T306A}$ similarly exhibits prolonged decay (τ_{fast} = 11.8 ± 0.5 s (72%) and τ_{slow} = 255 ± 153 s (28%); Figure S4F). Together, these results suggest that the incapability of Camuiα^{T286D} to integrate Ca^{2+} signals is not due to the inhibitory phosphorylation (Figure S3). Instead, our results suggest that active Thr286 phosphorylation is a prerequisite for CaMKII to integrate Ca^{2+} transients during sLTP induction.

The above results suggest that the impaired CaMKIIα^{T286A} activation during sLTP induction results from the fast decay of Camuiα^{T286A} activity (τ ~1.9 s), which is comparable to the interval of glutamate uncaging (~2 s). If this is the case, uncaging intervals shorter than the decay time should result in a higher degree of accumulation of CaMKII activity. As expected, when we applied higher frequency glutamate uncaging stimulations (1.9 Hz and 7.8 Hz), we found that CaMKIIα^{T286A} activity increased and plateaued at a significantly higher level in the stimulated spines (Figure 3A-3C) as well as in adjacent dendrite shafts (Figure 3D-3F). The decay time of Camuiα^{T286A} was comparable between different stimulation frequencies: τ_{decay} = 1.9 ± 0.7 s (1.9 Hz for 30 pulses, Figure 3A), τ_{decay} = 1.5 ± 1.0 s (1.9 Hz for 120 pulses, Figure 3B), and τ_{decay} = 3.1 ± 1.0 s (7.8 Hz for 120 pulses, Figure 3C). In comparison, τ_{decay} in wild-type CaMKIIα showed longer decay at all frequencies: τ_{fast} = 6.9 ± 0.5 s (81%) and τ_{slow} = 127 ± 84 s (19%) (1.9 Hz for 30 pulses, Figure 3A), τ_{fast} = 7.8 ± 0.9 s (69%) and τ_{slow} = 192 ± 132 s (31%) (1.9 Hz for 120 pulses, Figure 3B), and τ_{fast} = 7.2 ± 1.0 s (59%) and τ_{slow} = 103 ± 31 s (41%) (7.8 Hz for 120 pulses, Figure 3C). Our results indicate that even in the absence of Thr286

phosphorylation, CaMKIIα^{T286A} activity can be boosted by increasing the frequency of Ca^{2+} transients to rates that allow for their integration by CaMKIIα^{T286A}.

We next examined the role of Thr286 phosphorylation in sLTP. We measured structural plasticity in mEGFP-expressing CA1 pyramidal neurons of organotypic hippocampal slices prepared from *Camk2a*^{T286A} knock-in mice (Figure 4A-4G). We found that the sustained, but not the transient, phase of spine enlargement was significantly attenuated in *Camk2a*^{T286A} homozygous mice with the standard induction protocol (glutamate uncaging at 0.5 Hz, 30 pulses; $\Delta V_{sustained}$ = 16 ± 6% in *Camk2a*^{T286A} and $\Delta V_{sustained}$ = 89 ± 14% in littermate controls) (Figure 4A, 4B, 4F, 4G). Heterozygous mice exhibited a trend towards partial impairments in sLTP, although not statistically different ($\Delta V_{sustained}$ = 57 ± 11%) (Figure 4B, 4G).

If this impairment in sLTP is caused by the inability of CaMKIIα^{T286A} to integrate Ca^{2+} signals stimulated at this frequency, sLTP should be rescued by increasing the frequency of glutamate uncaging. Indeed, when sLTP is induced by 2 Hz glutamate uncaging (30 or 120 pulses), the partial sLTP impairment observed in heterozygous *Camk2a*^{T286A} mice was rescued ($\Delta V_{sustained}$ = 74.8 ± 14.9% for 2 Hz, 30 pulses and $\Delta V_{sustained}$ = 101.8 ± 21.4% for 2 Hz, 120 pulses; Figure 4C, 4D, 4G). Furthermore, structural plasticity in homozygous *Camk2a*^{T286} mice was fully rescued by 7.8 Hz glutamate uncaging (for 120 pulses) ($\Delta V_{sustained}$ = 85.2 ± 10.4%) (Figure 4E and 4G).

To confirm that sLTP induced by high frequency glutamate uncaging stimulation protocols is CaMKII-dependent, we transfected slices prepared from CaMKIIα conditional knock-out mice (*Camk2a*$^{fl/fl}$) (Hinds et al., 2003) with tdTomato fused Cre recombinase (tdTM-Cre) and mEGFP (or tdTM and mEGFP as a control). We found that tdTM-Cre transfected neurons displayed significant impairment in the sustained phase of spine enlargement (averaged over 25–30 min; $p < 0.05$) at all frequencies, while the transient phase (peak value recorded at 1 min) was partially blocked ($p < 0.05$; Figure S5A, S5B, S5C), consistent with the reported necessity of CaMKII activity to support the sustained phase of, but not the transient phase of sLTP (Lee et al., 2009; Matsuzaki et al., 2004). These results demonstrate that structural plasticity induced by high frequency glutamate uncaging is still CaMKIIα dependent.

To exclude the possibility that the rescue of sLTP is caused by CaMKIIβ activity, we knocked-down endogenous CaMKIIβ by shRNA and measured sLTP induced by 7.8 Hz glutamate uncaging (Figure S5D–H). CaMKIIβ knock-down partially inhibited sLTP when 0.5 Hz glutamate uncaging was used, suggesting that CaMKIIβ also regulates sLTP (Figure S5E, S5F) (Borgesius et al., 2011; Kim et al., 2015). However, normal sLTP was induced by 7.8 Hz glutamate uncaging in CA1 neurons of *Camk2a*^{T286A} mice expressing CaMKIIβ shRNA ($\Delta V_{sustained}$ = 94 ± 20 %) (Figure S5G, S5H). Thus, sLTP induced with high frequency in *Camk2a*^{T286A} is CaMKIIβ-independent.

In addition, to examine the possibility that the rescue of sLTP is caused by altered Ca^{2+} dynamics in the mutant mice, we measured Ca^{2+} elevations during sLTP induction (Figure S2). We found that Ca^{2+} dynamics in *Camk2a*^{T286A} were similar to that in WT, indicating

that Ca^{2+} transients are not affected in *Camk2a*^{T286A} mice. Taken together, the rescue of sLTP induced by high frequency glutamate uncaging is due to augmented CaMKIIα^{T286A} activity, by Ca^{2+} elevations elicited at higher frequency than CaMKIIα decay, in the stimulated spines.

Since it has been reported that overexpression of CaMKII^{T286D} affects spine structure and plasticity (Mayford et al., 1995; Pi et al., 2010a; Rotenberg et al., 1996), we quantified sLTP and basal spine size in neurons expressing Camuiα^{T286D}. While 0.49 Hz glutamate uncaging failed to induce sLTP in Camuiα^{T286D}-expressing neurons, 7.8 Hz glutamate uncaging fully rescued sLTP ($\Delta V_{sustained}$ = 71.6 ± 14.9 %) (Figure S5I, S5J). In addition, we observed a ~70% increase in the basal spine volume in neurons expressing Camuiα^{T286D} (Figure S5K, S5L), consistent with a previous study (Pi et al., 2010a).

Lastly, we investigated whether the impaired electrophysiological LTP in *Camk2a*^{T286A} mice could be rescued by high frequency electrical stimulation. To test this, we prepared acute hippocampal slices from *Camk2a*^{T286A} knock-in mice or littermate controls (4–5 weeks). We performed whole-cell patch clamp recordings from CA1 pyramidal neurons and measured EPSCs in response to stimulation of Schaffer collateral inputs. LTP was induced by pairing low frequency synaptic stimulation (2 Hz for 15 s) with postsynaptic depolarization to 0 mV. Assuming a ~20% release probability (Branco and Staras, 2009), 2 Hz presynaptic electrical stimulation corresponds to ~0.5 Hz glutamate uncaging, our standard sLTP protocol. While robust LTP was induced in wild-type neurons by this protocol (ΔEPSC = 96 ± 16 %), *Camk2a*^{T286A} neurons showed impaired LTP (ΔEPSC = 18 ± 10 %) (Figure 4H, 4I), in agreement with previous studies (Giese et al., 1998). However, when we applied high frequency synaptic stimulation (40 Hz, 15 s; corresponding to ~8 Hz glutamate uncaging), LTP in *Camk2a*^{T286A} mice was rescued (ΔEPSC = 76 ± 20%; Figure 4H, 4I). LTP induced by 40 Hz stimulation was abolished by the NMDAR antagonist APV, suggesting it is NMDAR-dependent (Figure S6A, S6B), unlike some other forms of LTP (Villers et al., 2014). To confirm that LTP induced by 40 Hz synaptic stimulation is CaMKII-dependent, we co-injected AAV encoding Cre and floxed-tdTM to the lateral ventricle of *Camk2a*$^{fl/fl}$ embryos. We prepared acute hippocampal slices at P21-P30, which were sparsely labeled with CaMKIIα KO CA1 hippocampal cells (see Supplemental Information). We found that LTP induced by 40 Hz synaptic stimulation was abolished in Cre- positive CA1 cells lacking CaMKIIα ($p < 0.05$; Figure S6C, S6D). Our results demonstrate that the impaired structural and electrophysiological LTP in CA1 neurons of *Camk2a*^{T286A} mice can be rescued by high frequency synaptic stimulation (paired with postsynaptic depolarization), which elicits peak activation of CaMKII^{T286A}. These results suggest phosphorylation at Thr286 significantly broadens the frequency domain over which CaMKII can integrate Ca^{2+} signals, and permits CaMKII to integrate Ca^{2+} signals at physiological relevant frequencies to induce synaptic plasticity.

DISCUSSION

In this study, we found that the rapid activation (~0.3 s) and the relatively slow decay (~6 s and ~1 min) of CaMKII underlie the stepwise activation, revealing its function as a leaky

biochemical integrator of Ca^{2+} signals. The integration window of CaMKII (6–8 s) also defines the frequency of stimulation required for inducing plasticity (Matsuzaki et al., 2004).

Our observations clarify the critical role of Thr286 phosphorylation in plasticity: it lowers the stimulation frequency required to induce synaptic plasticity, and permits CaMKII to integrate Ca^{2+} signals at physiologically relevant frequencies. The decay time of the non-phosphorylated mutant CaMKIIα^{T286A} and phospho-mimetic mutant CaMKIIα^{T286D} was ~3- and ~2-fold faster than that of wild-type CaMKII, respectively. The faster decay time of the mutants substantially compromised the integration capability of CaMKII for the same stimulation frequency. This result suggests that Thr286 phosphorylation is required for optimal integration of Ca^{2+} signals (Figure 2). The fast decay of CaMKIIα^{T286D} activity, perhaps due to the dissociation of Ca^{2+}/ CaM, suggests that dephosphorylation of Thr286 plays an important role in determining the optimum decay time (6 – 8 s) of CaMKII (but see also (Otmakhov et al., 2015)).

We also found that spine plasticity can be induced in *Camk2a*^{T286A} knock-in mice by increasing the frequency of stimulation. Our results indicate that peak CaMKIIα^{T286A} activity, achieved even without Thr286 phosphorylation, is able to relay Ca^{2+} signals to downstream molecules, such as Rho GTPase proteins, whose sustained activities have been shown to last > 30 min to support spine plasticity (Hedrick et al., 2016; Murakoshi et al., 2011; Nishiyama and Yasuda, 2015). Our findings suggest that Thr286 phosphorylation is dispensable for the maintenance of structural and elecrophysiological LTP, although prolonged Thr286 phosphorylation may occur during LTP under some conditions (Lengyel et al., 2004). Our results are consistent with previous studies demonstrating that inhibition of autonomous CaMKII activity inhibits LTP induction but does not impact LTP maintenance (Buard et al., 2010; Chen et al., 2001; Murakoshi et al., 2017). In addition, our results provide a molecular basis for the previous observation that Thr286 phosphorylation is required for rapid learning, but not memory (Irvine et al., 2005). Interestingly, structural plasticity can be also rescued by higher frequency glutamate uncaging in neurons expressing Camuiα^{T286D}. This result suggests that the net increase in CaMKII activity during sLTP induction is essential for synaptic plasticity (Bach et al., 1995; Mayford et al., 1995). Together, we provide evidence that CaMKIIα phosphorylation at Thr286 is not the biochemical trace of memory as previously suggested (Lisman et al., 2012). Instead, our findings demonstrate that Thr286 phosphorylation is essential for the optimal integration of Ca^{2+} signals, which is only required during plasticity induction.

STAR methods

CONTACT FOR REAGENT AND RESOURCE SHARING

Further information and requests for resources and reagents should be directed to and will be fulfilled by the Lead Contact, Ryohei Yasuda (ryohei.yasuda@mpfi.org).

EXPERIMENTAL MODEL AND SUBJECT DETAILS

All experimental protocols were approved by Max Planck Florida Institute IACUC, Duke University Medical Center or National Institutes of Natural Sciences and meet the guidelines of the National Institutes of Health guide for the Care and Use of Laboratory Animals.

Animals—Mice from BL6/C57 strain (purchased from Charles River Laboratories, both males and females) were used as wild-type group in 2pFLIM measurements. *Camk2a*^{T286A} knock-in mice were from Dr. KP. Giese (Giese et al., 1998). CaMKIIα conditional knock-out mice (*Camk2a*$^{fl/fl}$, strain name: C57BL/6-*Camk2a*^{tm1Vyb}; deposited by Dr. S. Tonegawa) that carry a floxed exon 2 allele were from the Jackson Laboratory (Hinds et al., 2003). All experimental animals were bred in-house under the animal care and guidelines of Duke University Medical Center and Max Planck Florida Institute for Neuroscience.

Hippocampal Slices—Organotypic cultured hippocampal slices were prepared from postnatal 4–7 day mice (both mail and females (see a detailed protocol at (Stoppini et al., 1991)). Briefly, tissue slices were plated on cell culture inserts (hydrophilic PTFE, 0.4 μm, Millipore) and maintained in tissue medium (minimum essential medium eagle (MEM) 8.4 mg/ml, horse serum 20%, L-glutamine 1 mM, $CaCl_2$ 1 mM, $MgSO_4$ 2 mM, D-glucose 12.9 mM, $NaHCO_3$ 5.2 mM, HEPES 30 mM, insulin 1 μg/ml, ascorbic acid 0.075%) at 37°C supplemented with 5% CO_2 until experiments (DIV 12–19). Hippocampal slices were biolistically transfected with plasmids at DIV 5–10 (12 mg gold particle, size: 1 μm, 30 μg plasmid). Acute slices were prepared from postnatal 30–40 day *Camk2a*^{T286A} mice and littermates. Preparation of slice cultures was in accordance with the animal care and guidelines of Duke University Medical Center and Max Planck Florida Institute for Neuroscience.

Acute Slices—Mice (both male and females) were sedated by isoflurane inhalation, and perfused intracardially with a chilled choline chloride solution. Brain was removed and placed in the same choline chloride solution composed of 124 mM Choline Chloride, 2.5 mM KCl, 26 mM $NaHCO_3$, 3.3 mM $MgCl_2$, 1.2 mM NaH_2PO_4, 10 mM glucose and 0.5 mM $CaCl_2$, pH 7.4 equilibrated with 95% O2/5% CO_2. Coronal slices (250 μm) were prepared from *Camk2a*^{T286A} mice and wild-type littermates age between P30-P40.

Primary Neuronal Culture—Neocortex dissected from 4 newborn mice (postnatal day 0; Both males and females) were triturated and plated into 35 mm dishes coated with 50 μg/ml PLL (Sigma) in culture medium composed of basal medium Eagle (BME) supplemented with 10% heat-inactivated fetal bovine serum (Invitrogen), 35 mM glucose (Sigma), 1 mM Glutamax (Sigma), 100 U/ml penicillin (Sigma), and 0.1 mg/ml streptomycin (Sigma). Proliferation of non-neuronal cells was inhibited by Cytosine arabinoside (2.5 μM) treatment on the second day after plating.

Method Details

Plasmids: Molecular cloning and mutations were carried out using QuikChange site-directed mutagenesis kit (Agilent Technologies) and InFusion cloning kit (Clontech). Expression of Camuiα was under pCAG promoter. Camuiα (dimVenus-CaMKII-mEGFP or

Green-Camuiα) was described previously (Lee et al, 2009). We used dimVenus ($Venus_{A208K, T145W}$) instead of sREACh, which has slightly better characteristics as FRET donor (Murakoshi et al., 2008), since this version has been already extensively characterized (Lee et al., 2009). shRNA against CaMKIIβ (*Mus musculus*) were purchased from GE-Dharmacon. pGIPZ *Camk2b* shRNA (TCAGAGAGGAACTTCCCAG; V2LMM2804) were used to knock-down *Camk2b*. pGIPZ non-silencing shRNA (CTTACTCTCGCCCAAGCGAGAG) were used as a control. pCMV-CaMKIIβ (*Rattus*) is from Dr. Hayashi (Okamoto et al, 2007).

Microscope—Fluorescent lifetime of Camuiα was measured by a home-built two-photon fluorescence lifetime imaging microscopy (2pFLIM). Camuiα was excited with a Ti:Sapphire laser tuned at 920 nm (Coherent, Chameleon) with laser power measured under the water immersion objective (Olympus, NA = 0.9, 60x) in the range of 1–1.5 mW, see detailed information at (Murakoshi et al., 2008; Yasuda et al., 2006). A second Ti:Sapphire laser at 720 nm (laser power measured under the objective: 2.5–3 mW), pulse duration of 4–6 ms was used to photolysis MNI-caged L-glutamate.

CaMKII activity imaging—Hippocampal slices were bathed in artificial cerebrospinal fluid (ACSF) bubbled with carbogen (95% O_2/ 5% CO_2) during the image recordings. Final ion concentrations (in mM) in imaging solution: NaCl 127, $NaHCO_3$ 25, D-glucose 25, KCl 2.5, NaH_2PO_4 1.25, supplemented with $CaCl_2$ 4, MNI-caged L-glutamate (Tocris) 4, TTX 0.001, Trolox (Sigma) 1. Between DIV 12–19, we imaged individual transfected CA1 pyramidal neurons. Dendritic spines on the secondary and tertiary apical dendrites were used for imaging. Images were acquired by a home-built 2pFLIM microscope controlled by custom software (MatLab). Experiments were performed at 25 ± 0.5°C or 34–35 °C as indicated. The temperature was controlled with a control syringe heater and an inline solution heater (TC344C, SW-10/6 and SH-27B, Warner Instruments). Recordings were performed with 32×32 pixels (pixel size: 12.3 ± 1.72 pixel/μm) at 128 ms/frame (7.8 Hz).

2pFLIM data analysis—Fluorescence lifetime of mEGFP in Camuiα is affected by the FRET efficiency. Fluorescence lifetime of mEGFP in Camuiα has at least 3 populations: closed conformation (basal), open conformation (active), and mEGFP (donor) with unfolded dimVenus (acceptor). The third population can be regarded as a constant component throughout the measurement. Since Camuiα is a monomeric FRET pair sensor (1:1 ratio of mEGFP: dimVenus), the change of mean fluorescence lifetime of Camuiα (τ_m) reflects the change of FRET efficiency and thus the conformation change of Camuiα. The mean fluorescence lifetime of Camuiα (τ_m) was derived from the mean photon arrival time $\langle t \rangle$ as follows:

$$\tau_m = \langle t \rangle - t_0 = \frac{\int \mathrm{dt} \cdot \mathrm{tF}(t)}{\int \mathrm{dt} \cdot F(t)} - t_0,$$

where $F(t)$ is the fluorescence lifetime decay curve and t_0 is the instrumental time offset. We estimated t_0 by fitting to the fluorescence decay curve summing all pixels in all frames over

a whole image session (typically 1024 frames) with a double exponential function convolved with the Gaussian pulse response function:

$$F(t)=F_0\sum_{i=1,2}P_iH(t,t_0,\tau_i,\tau_G),$$

where P_i is the population of fluorophore (mEGFP) with the fluorescence lifetime of τ_i, respectively, and $H(t)$ is the fluorescence lifetime curve with a single exponential function convolved with the Gaussian pulse response function:

$$H(t,t_0,\tau_i,\tau_G)=\frac{1}{2}\exp\left(\frac{\tau_G^2}{2\tau_i^2}-\frac{t-t_0}{\tau_i}\right)\mathrm{erfc}\left(\frac{\tau_G^2-\tau_i(t-t_0)}{\sqrt{2}\tau_i\tau_G}\right)-t_0^{'},$$

in which τ_G is the width of the Guassian pulse response function, F_0 is the peak fluorescence before convolution, $t_0^{'}$ is the instrumental time offset measured by the fitting, and erfc is the error function. Since the mean fluorescence lifetime can be obtained from the fitting as

$$\tau_m=\frac{\sum_i P_i\tau_i^2}{\sum_i P_i\tau_i}$$

t_0 can be calculated as:

$$t_0=\langle t\rangle-\frac{\sum_i P_i\tau_i^2}{\sum_i P_i\tau_i}$$

In our typical setting, t0 is ~ 1–2 ns. For Green-Camuiα, the parameters are typically, τ1 ~ 1.9–2.1 ns, τ2 ~ 0.4–0.6 ns, τG ~ 0.15 ns and P1 ~ 0.4–0.5 (P2 = 1 − P1). A change in the population (P1 and P2) by ~ 10% causes a change in the mean fluorescence lifetime (τm) by ~ 0.1 ns.. A change in the population (P_1 and P_2) by ~ 10% causes a change in the mean fluorescence lifetime (τ_m) by ~ 0.1 ns. It should be noted that changes in the fluorescence lifetime are independent of the fitting.

Measurements of structural plasticity—Two-photon laser scanning microscopy (2pLSM) was used to quantify the spine volume change during glutamate uncaging of sLTP (Matsuzaki et al., 2004). When the experiments were performed in *Camk2a* ^{T286A} knock-in mice, hippocampal slices were cultured from *Camk2a*$^{T286A/T286A}$ (homozygous), *Camk2a*$^{T286A/WT}$ (heterozygous), and wild-type littermates. Hippocampal slices were biolistically transfected with mEGFP (12 mg gold particle, size: 1 μm, 30 μg plasmid) at DIV 7–10. Transfected CA1 neurons were imaged between DIV 12–17. For the experiments performed in *Camk2a*$^{fl/fl}$ mice, the transfected plasmids are as follows: 1) conditional knock-out group: co-transfected with tdTomato labeled Cre recombinase (pCAG-tdTM-cre, 25 μg) and mEGFP (pCAG-mEGFP, 20 μg); 2) control group: co-transfected with tdTomato (pCAG-tdTM, 25 μg) and pCAG-mEGFP (20 μg). Transfected CA1 neurons with Cre positive cells were excited with Ti:Sapphire laser at 920 nm (Coherent, Chameleon) with

laser power measured under the objective (Olympus, NA = 0.9, 60x) in the range of 1–1.5 mW. Green-channel fluorescence collected from PMT (photoelectron multiplier tubes) placed after the 510 nm/70 nm (bandwidth) wavelength filters were used for spine volume change analysis.

Calcium imaging—We performed whole-cell patch clamp to hippocampal cultured neurons from *Camk2a*^{T286A} mice and wild-type littermates with the pipette containing Fluo-4FF (Ca^{2+} indicator) and Alexa-594 in Potassium Gluconate internal solution (in mM: K gluconate 130, Na phosphocreatine 10, MgCl2 4, Na_2ATP 4, MgGTP 0.3, L- Ascorbic acid 3, HEPES 10, pH 7.4, 310 mosm). 2pLSM and Ti:Sapphire laser at 920 nm (Coherent, Chameleon) was used to simultaneously excite the two fluorescent dyes and thus the fluorescence from Fluo-4FF can be used to quantify the [Ca^{2+}] transients during glutamate uncaging of sLTP. Images were acquired every 64 ms.

AAV injection—E14.5/15.5 timed-pregnant *Camk2a*$^{fl/fl}$ mice were anesthetized with ~2% isoflurane and administered 0.1 mg buprenorphine SR (ZooPharm) for analgesia. The uterine horns were exposed through an abdominal incision and the right lateral ventricle of each embryo was injected with approximately 1–2 μl of AAV solution. Half of the embryos were injected with AAV1.CAG.EGFP, and half were injected with AAV1.CAG.Flex.tdTomato/ AAV1.hSyn.Cre (all from U Penn vector core).

Electrophysiology—Slices were maintained in a submerged chamber at 32 °C for 1h and then at room temperature in oxygenated ACSF. Whole cell recordings and LTP protocol: CA1 pyramidal neurons were visualized using oblique illumination. Whole cell recordings were performed using a patch-clamp amplifier (Multiclamp 700B, Molecular Devices). Patch pipettes (3–6 ΩM) were filled with a K Gluconate solution (130 mM K gluconate, 10 mM Na phosphocreatine, 4 mM $MgCl_2$, 4 mM Na_2ATP, 0.3 mM MgGTP, 3 mM L-Ascorbic acid, 10 mM HEPES, pH 7.4, 310 mosm). Series resistances (10 to 40 MΩ) and input resistances (100 to 300 MΩ) were monitored throughout the experiment using negative voltage steps (-5 mV, 50 ms). The membrane potential was held at −70 mV. Experiments were performed at room temperature and slices were perfused with oxygenated ACSF (127 mM NaCl, 2.5 mM KCl, 10 mM glucose, 10 mM $NaHCO_3$, 1.25 mM NaH_2PO_4, 2 mM $MgCl_2$, 2 mM $CaCl_2$, 0.1 mM Picrotoxin). Excitatory postsynaptic currents (EPSCs) were evoked by extracellular stimulation of the Schaffer collateral fibers using a concentric bipolar stimulating electrode (World Precision Instruments) at 0.03 Hz. LTP was induced by pairing synaptic stimulation (2 Hz for 120 pulses, or 40 Hz for 600 pulses at the end of the depolarization) with a postsynaptic depolarization to 0 mV (60 s). EPSP potentiation was assessed for 50–60 min after LTP condition stimulation. For the APV experiments, APV (50 μM) was applied 10 min before recording. All data was analyzed with an in-house program written in MatLab.

Validation of shRNA—Dissociated cortical neuron cultures were infected with GIPZ lentiviral CAMKIIβ shRNA (1 μl/ml) or GIPZ lentiviral scramble shRNA (titer: 1.5×1013 genome copies/μl; Dharmacon) at DIV 6. On DIV 14–16, neurons were washed with PBS and immediately extracted with SDS buffer. Samples were separated on 4–20% acrylamide

gel (Mini-PROTEAN TGX precast gels, Bio-Rad), then transferred onto 0.45 μm pore size PVDF membranes (Millipore) using semidry immunoblotting (transfer buffer containing 25 mM Tris, 200 mM glycine and 20% methanol). Membranes were blocked with 5% nonfat milk in TBS-T (Tris Buffered Saline with 0.1% Tween-20) for 1 hour at room temperature, then incubated overnight at 4°C with primary antibodies diluted in 5% BSA in TBS-T. We used the following commercially available antibodies: mouse anti-CAMKIIβ (1:200; LS-B5767; LSBio), and mouse anti-β-actin (1:2000; Sigma). Membranes were washed 3 times for 15 minutes in TBS-T, followed by incubation for 1 hour at room temperature with HRP-conjugated rabbit anti-mouse secondary antibody (Bio-Rad), diluted 1:2000 in 5% nonfat milk in TBS-T. Membranes were washed 3 times for 15 minutes in TBS-T, then incubated with Pierce ECL Plus western blotting substrate (for CAMKIIβ) or Pierce ECL western blotting substrate (for β-actin) to detect western blotted proteins. We used the Image Quant LAS4000 Imaging System (GE Healthcare) to visualize protein bands. Image J software was used to quantify endogenous CAMKIIβ levels normalized to β-actin to ensure equal loading.

The Quantification and Statistical Analysis—Error bars shown in the figures represent standard error of the mean (s.e.m). One-way ANOVA analysis with *post hoc* Bonferroni test are used to compare different conditions ($\alpha = 0.05$). *n* indicates the number of spines/neurons for spine imaging results and the number of cells for electrophysiology results. Asterisks denote the statistical significance ($^*p < 0.05$). s.e.m of time constants is obtained by bootstrapping.

Supplementary Material

Refer to Web version on PubMed Central for supplementary material.

Acknowledgments

We thank Dr. K.P. Giese for *Camk2a*^{T286A} mice and Dr. S. Tonegawa for *Camk2a*$^{fl/fl}$ mice (through Jackson lab). We thank Dr. L. Yan for advice and instructions on the optics. We thank members of the Yasuda lab for discussion, and T. Yasuda, Dr. C. Yokoyama, Dr. P. Evans and Dr. L. Colgan for the critical reading of the manuscript. We also thank M. Hu and J. Richards for preparing cultured slices and D. Kloetzer for laboratory management. This study was funded by NIH (R01MH080047 and 1DP1NS096787).

References

Bach ME, Hawkins RD, Osman M, Kandel ER, Mayford M. Impairment of spatial but not contextual memory in CaMKII mutant mice with a selective loss of hippocampal LTP in the range of the theta frequency. Cell. 1995; 81:905–915. [PubMed: 7781067]

Barria A, Muller D, Derkach V, Griffith LC, Soderling TR. Regulatory phosphorylation of AMPA-type glutamate receptors by CaM-KII during long-term potentiation. Science. 1997; 276:2042–2045. [PubMed: 9197267]

Borgesius NZ, van Woerden GM, Buitendijk GH, Keijzer N, Jaarsma D, Hoogenraad CC, Elgersma Y. betaCaMKII plays a nonenzymatic role in hippocampal synaptic plasticity and learning by targeting alphaCaMKII to synapses. J Neurosci. 2011; 31:10141–10148. [PubMed: 21752990]

Branco T, Staras K. The probability of neurotransmitter release: variability and feedback control at single synapses. Nat Rev Neurosci. 2009; 10:373–383. [PubMed: 19377502]

Buard I, Coultrap SJ, Freund RK, Lee YS, Dell'Acqua ML, Silva AJ, Bayer KU. CaMKII "autonomy" is required for initiating but not for maintaining neuronal long-term information storage. J Neurosci. 2010; 30:8214–8220. [PubMed: 20554872]

Chao LH, Stratton MM, Lee IH, Rosenberg OS, Levitz J, Mandell DJ, Kortemme T, Groves JT, Schulman H, Kuriyan J. A mechanism for tunable autoinhibition in the structure of a human Ca2+/calmodulin- dependent kinase II holoenzyme. Cell. 2011; 146:732–745. [PubMed: 21884935]

Chen HX, Otmakhov N, Strack S, Colbran RJ, Lisman JE. Is persistent activity of calcium/calmodulin-dependent kinase required for the maintenance of LTP? J Neurophysiol. 2001; 85:1368–1376. [PubMed: 11287461]

De Koninck P, Schulman H. Sensitivity of CaM kinase II to the frequency of Ca2+ oscillations. Science. 1998; 279:227–230. [PubMed: 9422695]

Fujii H, Inoue M, Okuno H, Sano Y, Takemoto-Kimura S, Kitamura K, Kano M, Bito H. Nonlinear decoding and asymmetric representation of neuronal input information by CaMKIIalpha and calcineurin. Cell Rep. 2013; 3:978–987. [PubMed: 23602566]

Giese KP, Fedorov NB, Filipkowski RK, Silva AJ. Autophosphorylation at Thr286 of the alpha calcium-calmodulin kinase II in LTP and learning. Science. 1998; 279:870–873. [PubMed: 9452388]

Hanson PI, Kapiloff MS, Lou LL, Rosenfeld MG, Schulman H. Expression of a multifunctional Ca2+/calmodulin-dependent protein kinase and mutational analysis of its autoregulation. Neuron. 1989; 3:59–70. [PubMed: 2619995]

Hanson PI, Meyer T, Stryer L, Schulman H. Dual role of calmodulin in autophosphorylation of multifunctional CaM kinase may underlie decoding of calcium signals. Neuron. 1994; 12:943–956. [PubMed: 8185953]

Hedrick NG, Harward SC, Hall CE, Murakoshi H, McNamara JO, Yasuda R. Rho GTPase complementation underlies BDNF-dependent homo- and heterosynaptic plasticity. Nature. 2016; 538:104–108. [PubMed: 27680697]

Hinds HL, Goussakov I, Nakazawa K, Tonegawa S, Bolshakov VY. Essential function of alpha-calcium/calmodulin-dependent protein kinase II in neurotransmitter release at a glutamatergic central synapse. Proc Natl Acad Sci U S A. 2003; 100:4275–4280. [PubMed: 12629219]

Irvine EE, Vernon J, Giese KP. AlphaCaMKII autophosphorylation contributes to rapid learning but is not necessary for memory. Nat Neurosci. 2005; 8:411–412. [PubMed: 15778710]

Kim K, Lakhanpal G, Lu HE, Khan M, Suzuki A, Hayashi MK, Narayanan R, Luyben TT, Matsuda T, Nagai T, et al. A Temporary Gating of Actin Remodeling during Synaptic Plasticity Consists of the Interplay between the Kinase and Structural Functions of CaMKII. Neuron. 2015; 87:813–826. [PubMed: 26291163]

Lee SJ, Escobedo-Lozoya Y, Szatmari EM, Yasuda R. Activation of CaMKII in single dendritic spines during long-term potentiation. Nature. 2009; 458:299–304. [PubMed: 19295602]

Lengyel I, Voss K, Cammarota M, Bradshaw K, Brent V, Murphy KP, Giese KP, Rostas JA, Bliss TV. Autonomous activity of CaMKII is only transiently increased following the induction of long-term potentiation in the rat hippocampus. Eur J Neurosci. 2004; 20:3063–3072. [PubMed: 15579161]

Lisman J, Yasuda R, Raghavachari S. Mechanisms of CaMKII action in long-term potentiation. Nat Rev Neurosci. 2012; 13:169–182. [PubMed: 22334212]

Malinow R, Schulman H, Tsien RW. Inhibition of postsynaptic PKC or CaMKII blocks induction but not expression of LTP. Science. 1989; 245:862–866. [PubMed: 2549638]

Matsuzaki M, Honkura N, Ellis-Davies GC, Kasai H. Structural basis of long-term potentiation in single dendritic spines. Nature. 2004; 429:761–766. [PubMed: 15190253]

Mayford M, Wang J, Kandel ER, O'Dell TJ. CaMKII regulates the frequency-response function of hippocampal synapses for the production of both LTD and LTP. Cell. 1995; 81:891–904. [PubMed: 7781066]

Murakoshi H, Lee SJ, Yasuda R. Highly sensitive and quantitative FRET-FLIM imaging in single dendritic spines using improved non-radiative YFP. Brain Cell Biol. 2008; 36:31–42. [PubMed: 18512154]

Murakoshi H, Shin ME, Parra-Bueno P, Szatmari EM, Shibata AC, Yasuda R. Kinetics of Endogenous CaMKII Required for Synaptic Plasticity Revealed by Optogenetic Kinase Inhibitor. Neuron. 2017; 94:37–47. e35. [PubMed: 28318784]

Murakoshi H, Wang H, Yasuda R. Local, persistent activation of Rho GTPases during plasticity of single dendritic spines. Nature. 2011; 472:100–104. [PubMed: 21423166]

Nishiyama J, Yasuda R. Biochemical Computation for Spine Structural Plasticity. Neuron. 2015; 87:63–75. [PubMed: 26139370]

Okamoto K, Narayanan R, Lee SH, Murata K, Hayashi Y. The role of CaMKII as an F-actin-bundling protein crucial for maintenance of dendritic spine structure. Proc Natl Acad Sci U S A. 2007; 104:6418–6423. [PubMed: 17404223]

Opazo P, Labrecque S, Tigaret CM, Frouin A, Wiseman PW, De Koninck P, Choquet D. CaMKII triggers the diffusional trapping of surface AMPARs through phosphorylation of stargazin. Neuron. 2010; 67:239–252. [PubMed: 20670832]

Otmakhov N, Griffith LC, Lisman JE. Postsynaptic inhibitors of calcium/calmodulin-dependent protein kinase type II block induction but not maintenance of pairing-induced long-term potentiation. J Neurosci. 1997; 17:5357–5365. [PubMed: 9204920]

Otmakhov N, Regmi S, Lisman JE. Fast Decay of CaMKII FRET Sensor Signal in Spines after LTP Induction Is Not Due to Its Dephosphorylation. PLoS One. 2015; 10:e0130457. [PubMed: 26086939]

Pi HJ, Otmakhov N, El Gaamouch F, Lemelin D, De Koninck P, Lisman J. CaMKII control of spine size and synaptic strength: role of phosphorylation states and nonenzymatic action. Proc Natl Acad Sci U S A. 2010a; 107:14437–14442. [PubMed: 20660727]

Pi HJ, Otmakhov N, Lemelin D, De Koninck P, Lisman J. Autonomous CaMKII can promote either long-term potentiation or long-term depression, depending on the state of T305/T306 phosphorylation. J Neurosci. 2010b; 30:8704–8709. [PubMed: 20592192]

Rotenberg A, Mayford M, Hawkins RD, Kandel ER, Muller RU. Mice expressing activated CaMKII lack low frequency LTP and do not form stable place cells in the CA1 region of the hippocampus. Cell. 1996; 87:1351–1361. [PubMed: 8980240]

Sanhueza M, Fernandez-Villalobos G, Stein IS, Kasumova G, Zhang P, Bayer KU, Otmakhov N, Hell JW, Lisman J. Role of the CaMKII/NMDA receptor complex in the maintenance of synaptic strength. J Neurosci. 2011; 31:9170–9178. [PubMed: 21697368]

Sanhueza M, McIntyre CC, Lisman JE. Reversal of synaptic memory by Ca2+/calmodulin-dependent protein kinase II inhibitor. J Neurosci. 2007; 27:5190–5199. [PubMed: 17494705]

Shen K, Teruel MN, Connor JH, Shenolikar S, Meyer T. Molecular memory by reversible translocation of calcium/calmodulin-dependent protein kinase II. Nat Neurosci. 2000; 3:881–886. [PubMed: 10966618]

Stoppini L, Buchs PA, Muller D. A simple method for organotypic cultures of nervous tissue. J Neurosci Methods. 1991; 37:173–182. [PubMed: 1715499]

Takao K, Okamoto K, Nakagawa T, Neve RL, Nagai T, Miyawaki A, Hashikawa T, Kobayashi S, Hayashi Y. Visualization of synaptic Ca2+ /calmodulin-dependent protein kinase II activity in living neurons. J Neurosci. 2005; 25:3107–3112. [PubMed: 15788767]

Villers A, Giese KP, Ris L. Long-term potentiation can be induced in the CA1 region of hippocampus in the absence of alphaCaMKII T286-autophosphorylation. Learn Mem. 2014; 21:616–626. [PubMed: 25322797]

Walkup, WGt, Washburn, L., Sweredoski, MJ., Carlisle, HJ., Graham, RL., Hess, S., Kennedy, MB. Phosphorylation of synaptic GTPase-activating protein (synGAP) by Ca2+/calmodulin-dependent protein kinase II (CaMKII) and cyclin-dependent kinase 5 (CDK5) alters the ratio of its GAP activity toward Ras and Rap GTPases. J Biol Chem. 2015; 290:4908–4927. [PubMed: 25533468]

Yagishita S, Hayashi-Takagi A, Ellis-Davies GC, Urakubo H, Ishii S, Kasai H. A critical time window for dopamine actions on the structural plasticity of dendritic spines. Science. 2014; 345:1616–1620. [PubMed: 25258080]

Yang Y, Tao-Cheng JH, Bayer KU, Reese TS, Dosemeci A. Camkii-mediated phosphorylation regulates distributions of Syngap-alpha1 and -alpha2 at the postsynaptic density. PLoS One. 2013; 8:e71795. [PubMed: 23967245]

Yasuda R, Harvey CD, Zhong H, Sobczyk A, van Aelst L, Svoboda K. Supersensitive Ras activation in dendrites and spines revealed by two-photon fluorescence lifetime imaging. Nat Neurosci. 2006; 9:283–291. [PubMed: 16429133]

In brief

Chan et al. showed that CaMKII activation acts as a leaky integrator of Ca2+ pulses in dendritic spines, and demonstrated that phosphorylation of T286 is necessary for optimal integration of Ca^{2+} pulses during the induction of LTP but dispensable for the maintenance of LTP.

Highlights

- CaMKII acts as a leaky integrator of Ca^{2+} pulses in dendritic spines
- Phosphorylation at T286 is necessary for optimal integration of Ca^{2+} pulses
- Phosphorylation at T286 is dispensable for the maintenance of LTP

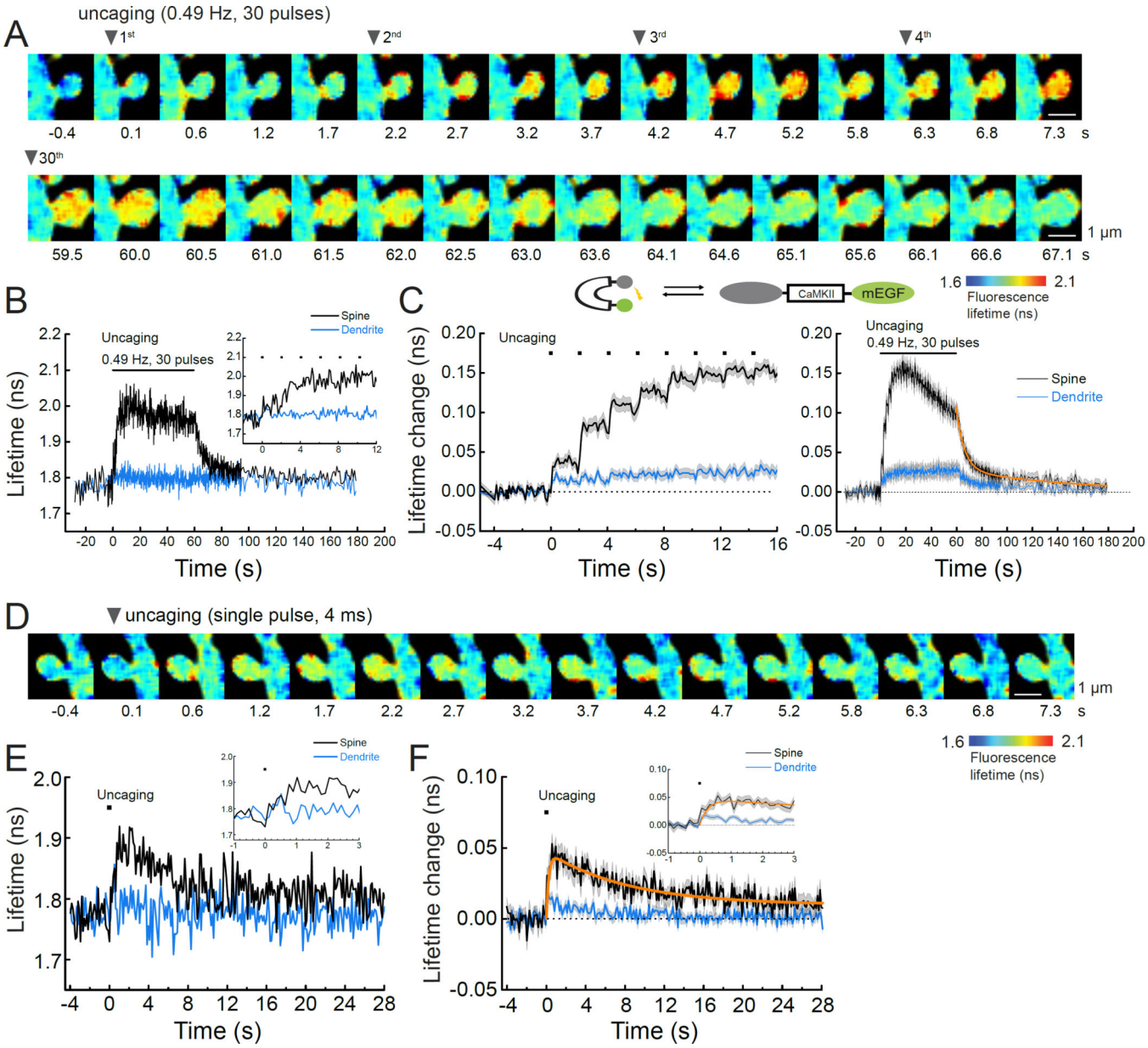

Figure 1. CaMKII Activation Measured with Millisecond Temporal Resolution

(A) Representative fluorescence lifetime images of Camuiα during glutamate uncaging at 0.49 Hz. Warmer colors indicate higher fluorescence lifetime of Camuiα, corresponding to the active, open conformation of Camuiα.

(B) Time course of fluorescence lifetime of Camuiα in (A) of the stimulated spine (black) and dendritic region (blue). Inset is expanded view of the rising phase of Camuiα activation. Black dots represent uncaging pulses.

(C) Averaged change in fluorescence lifetime of Camuiα (n = 36 spines/14 neurons). Left panel is expanded view of the rising phase of right panel. The orange curve indicates the decay kinetics of fluorescence lifetime signal obtained by curve fitting of a double-exponential function: $F(t) = F_0 \blacksquare [P_{fast} \blacksquare e^{-t/\tau fast} + P_{slow} \blacksquare e^{-t/\tau slow}]$, where F_0 is the initial fluorescence lifetime, τ_{fast} and τ_{slow} are the fast and slow decay time constants and P_{fast} and

P_{slow} are the respective populations. The time constants are obtained as τ_{fast} = 6.4 ± 0.7 s (P_{fast} = 74%) and τ_{slow} = 92.6 ± 50.7 s (P_{slow} = 26%).

(D) Representative fluorescence lifetime images of Camuiα in response to a single glutamate uncaging pulse.

(E) Time course of fluorescence lifetime of Camuiα in (D).

(F) Averaged change in fluorescence lifetime of Camuiα (n = 35 spines/8 neurons) in response to a single glutamate uncaging pulse. The orange curve indicates the kinetics of fluorescence lifetime signal obtained by curve fitting of a function: $F(t) = [a \blacksquare e^{-t/\tau fast} + c] \blacksquare [1- e^{-t/\tau rise}]$, where c is a constant which represents the slow decay component as described in (C). The time constants are obtained as: τ_{rise} = 0.3 ± 0.1 s and τ_{fast} = 8.2 ± 1.7 s. All data are shown in mean ± s.e.m., and s.e.m. of time constants is obtained by bootstrapping. Scale bar, 1 μm.

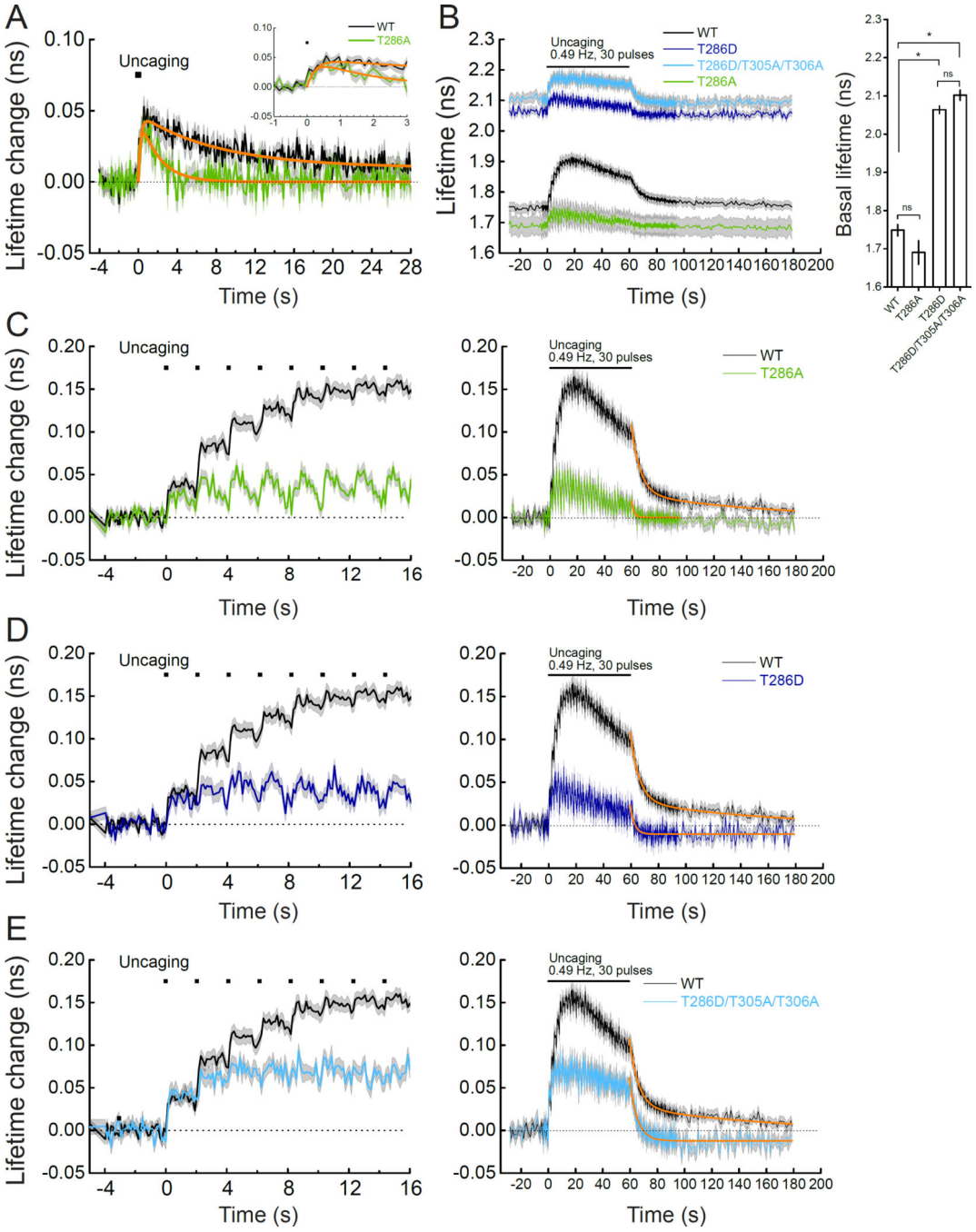

Figure 2. Activation of Camuiα^{T286A} and Camuiα^{T286A} During sLTP Induction

(A) Activation of Camuiα^{T286A} (green) and Camuiα^{WT} (black) in response to a single glutamate uncaging pulse (black dot). The data and fitted curve for Camuiα^{WT} are from Figure 1F for comparison. The orange curve on Camuiα^{T286A} indicates the decay kinetics obtained by curve fitting of a function: $F(t) = C \blacksquare [1 - e^{-t/\tau rise}] \blacksquare e^{-t/\tau decay}$, where τ_{rise} is adapted from Figure 1F and is fixed during curve fitting (τ_{rise} = 0.3 s). The decay time constant for Camuiα^{T286A} is 1.9 ± 0.3 s (n = 30 spines/9 neurons). Inset is expanded view of the rising phase of Camuiα^{T286A} activation.

(B) Averaged fluorescence lifetime of Camuiα^{WT} , Camuiα^{T286A} , Camuiα^{T286D} , and Camuiα$^{T286D/T305A/T306A}$ during sLTP induction. Right panel is fluorescence lifetime averaged over −4–0 s: Camuiα^{WT}: 1.75 ± 0.02 ns; Camuiα^{T286A}: 1.69 ± 0.03 ns; Camuiα^{T286D}: 2.06 ± 0.01 ns; Camuiα$^{T286/T305A/T306A}$: 2.10 ± 0.01 ns. Asterisks denote the statistical significance ($p < 0.05$; ANOVA followed by *post hoc* Bonferroni test). (C–E) Averaged change in fluorescence lifetime of Camuiα^{T286A} (C; green), Camuiα^{T286D} (D; navy), Camuiα$^{T286D/T305A/T306A}$ (E; light blue) and Camuiα^{WT} (black) in the stimulated spine during glutamate uncaging. The data and fitted curve for Camuiα^{WT} are from Figure 1C for comparison. Left panel is expanded view of the right panel. The orange curve on Camuiα^{T286A} is obtained by curve fitting of a function: $F(t) = C \cdot e^{-t/\tau_{decay}}$. The decay time constant is obtained as 1.9 ± 1.2 s (26 spines/12 neurons). The orange curve on Camuiα^{T286D} and Camuiα$^{T286D/T305A/T306A}$ are obtained by curve fitting of a function: $F(t) = C \cdot e^{-t/\tau_{decay}} + d_0$, where d_0 is a constant. The decay time constant is obtained as 3.0 ± 0.6 s for Camuiα^{T286D} (33 spines/10 neurons) and 5.7 ± 0.5 s for Camuiα$^{T286D/T305A/T306A}$ (32 spines/7 neurons). All data are shown in mean ± s.e.m., and s.e.m. of time constants is obtained by bootstrapping.

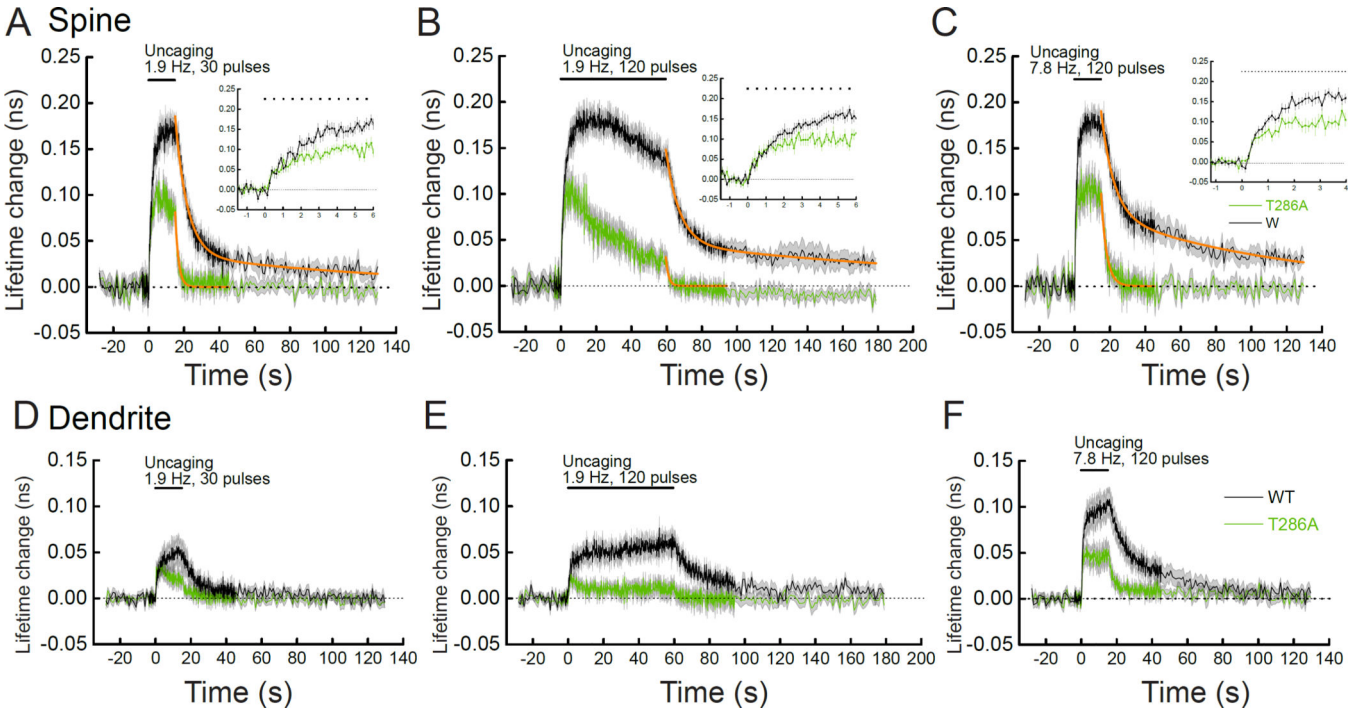

Figure 3. CaMKII Activation in Dendritic Spines in Response to High-frequency Glutamate Uncaging

(A–C) Averaged change in fluorescence lifetime of Camuiα^{WT} (black) and Camuiα^{T286A} (green) in response to high frequency glutamate uncaging at 1.9 Hz (A, B) or 7.8 Hz (C) for 30 pulses (A) or 120 pulses (B, C) in the dendritic spines. Insets are expanded view. The orange curves indicate the decay kinetics obtained by a double-exponential fitting for Camuiα^{WT} (see details in Figure 1C) and mono-exponential fitting for Camuiα^{T286A} (see details in Figure 2C). The obtained decay time constants are as follows (number of samples: spines/neurons): (A) Camuiα^{WT}: τ_{fast} = 6.9 ± 0.5 s (81%) and τ_{slow} = 127 ± 84 s (19%) (21/14). Camuiα^{T286A}: τ_{decay} = 1.9 ± 0.7 s (22/16). (B) Camuiα^{WT}: τ_{fast} = 7.8 ± 0.9 s (69%) and τ_{slow} = 192 ± 132 s (31%) (18/11). Camuiα^{T286A}: τ_{decay} = 1.5 ± 1.0 s (17/10). (C) Camuiα^{WT}: τ_{fast} = 7.2 ± 1.0 s (59%) and τ_{slow} = 103 ± 31 s (41%) (25/13). Camuiα^{T286A}: τ_{decay} = 3.1 ± 1.0 s (15/8).

(D–F) Averaged change in fluorescence lifetime in dendritic region as shown in (A–C), respectively. All data are shown in mean ± s.e.m., and s.e.m. of time constants is obtained by bootstrapping.

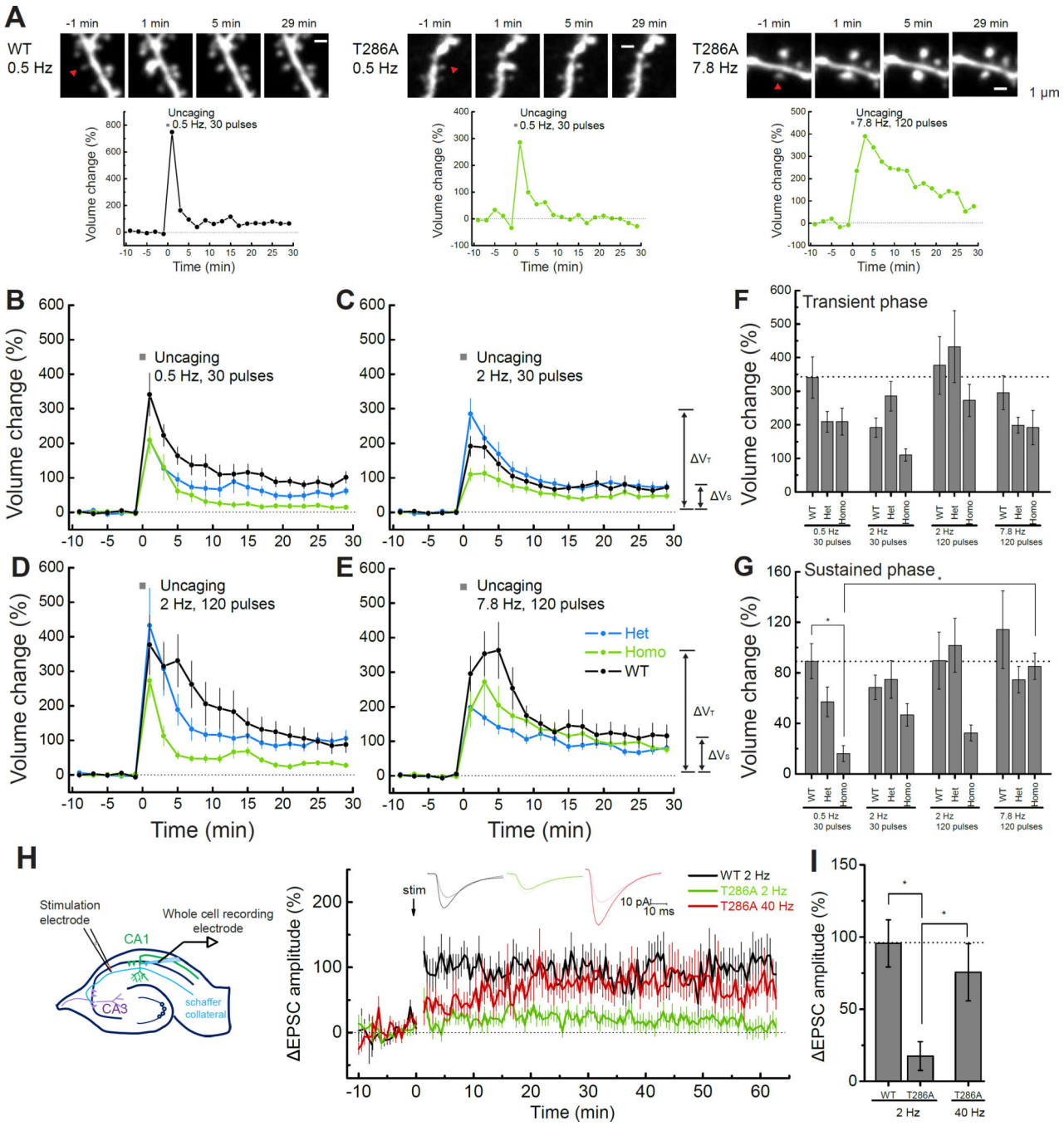

Figure 4. Structural and Electrophysiological Plasticity Induced by High Frequency Stimulation

(A) Fluorescence intensity images (mEGFP) of spine structural plasticity during sLTP. The arrowhead indicates the spot of two-photon glutamate uncaging. Scale bar, 1 μm.

(B–E) Structural LTP of neurons from *Camka*^{T286A} wild-type (WT/WT), heterozygous (WT/T286A) or homozygous (T286A/T286A) mice induced by glutamate uncaging at 0.5 Hz for 30 pulses (B), 2 Hz for 30 pulses (C), 2 Hz for 120 pulses (D) or 7.8 Hz for 120 pulses (E). Number of samples (spines/neurons) are 22/22 for WT, 27/26 for Het, and 25/25 for Homo in (B); 17/16 for WT, 18/18 for Het, and 12/12 for Homo in (C); 15/15 for WT,

13/13 for Het, and 14/14 for Homo in (D), and 15/15 for Homo, 20/19 for Het, and 16/16 for Homo in (E).

(F–G) Quantifications of spine volume change during the transient phase (F; peak value recorded at 1 min) or the sustained phase (G; averaged over 25–30 min). Asterisks denote the statistical significance ($p < 0.05$; ANOVA followed by *post hoc* Bonferroni test).

(H) Whole-cell recording of LTP induced at the Schaffer collateral in CA1 neurons from *Camk2a*^{T286A} and litter-mate control mice. LTP is induced by electrical stimulations at 2 Hz for 60 s or 40 Hz for 15 s with depolarization to 0 mV. Number of neurons is 19 for WT, 20 for T286A (2 Hz) and 27 for T286A (40 Hz). Typical EPSC traces before (-5–0 min) and after (43–63 min) are presented on top of the panel.

(I) Quantification of EPSC potentiation averaged over 40 – 63 min. Asterisks denote the statistical significance ($p < 0.05$; ANOVA followed by *post hoc* Bonferroni test). All data are shown in mean ± s.e.m.

REAGENT or RESOURCE	SOURCE	IDENTIFIER
Antibodies		
Anti-CaMKIIβ	LSBio	Cat# LS-B5767-50, RRID: AB_10915143
Anti-Actin	Sigma	Cat# A5316 RRID: AB_476743
Bacterial and Virus Strains		
AAV1.CAG.Flex.tdTomato	University of Pennsylvania Vector Core	N/A
AAV1.hSyn.Cre	University of Pennsylvania Vector Core	N/A
pGIPZ *Camk2b* shRNA	GE-Dharmacon	Cat# VGM5524 Source Clone ID: V2LMM_2804
pGIPZ non-silencing shRNA	GE-Dharmacon	Cat# RHS4348
Biological Samples		
Chemicals, Peptides, and Recombinant Proteins		
MNI-caged-L-glutamate	Tocris	Cat# 1490
Tetrodotoxin	Tocris	Cat# 1078
MEM	Sigma-Aldrich	Cat# M4642
Critical Commercial Assays		
Pierce BCA Protein Assay Kit	Thermo Scientific	Cat# 23225
Deposited Data		
Experimental Models: Cell Lines		
Experimental Models: Organisms/Strains		
Mouse- C57BL/6NCrl	Charles River	Strain Code: 027
Mouse- *Camk2a*$^{T286A/T286A}$	Giese et al. 1998	Dr. K. Peter-Giese
Mouse- *Camk2a*$^{fl/fl}$ C57BL/6-*Camk2a*^{tm1Vyb}	Hinds et al., 2003	Jackson lab, Stock # 006575
Oligonucleotides		
Recombinant DNA		
Camuiα (Green-Camuiα or Venus$_{A208K,T145W}$-CaMKIIα- mEGFP)	Lee et al., 2009	N/A
pCMV-CaMKIIβ (*Rattus*)	Okamoto et al., 2007	Dr. Y. Hayashi
Software and Algorithms		
Prism 6	GraphPad Software	https://www.graphpad.com/scientific-software/prism/
Matlab	MathWorks	https://www.mathworks.com/
Other		
Millicell Cell Culture Insert, 30 mm, hydrophilic PTFE, 0.4 μm	EMD Millipore	Cat# PICM0RG50